Available online at www.sciencedirect.com
ScienceDirect
Journal of Photochemistry and Photobiology A: Chemistry 187 (2007) 305–310
Journal of Photochemistry and Photobiology A:Chemistry
www.elsevier.com/locate/jphotochem

The charge transfer mechanism and spectral properties of a near-infrared heptamethine cyanine dye in alcoholic and aprotic solvents

Li-Chuan Zhou [a], Guang-Jiu Zhao [a], Ji-Feng Liu [a], Ke-Li Han [a,*], Yun-Kou Wu [b], Xiao-Jun Peng [b], Meng-Tao Sun [c]

[a] *State Key Lab of Molecular Reaction Dynamics, Dalian Institute of Chemical Physics, Chinese Academy of Sciences, Dalian 116023, China*
[b] *State Key Laboratory of Fine Chemicals, Dalian University of Technology, 158 Zhongshan Road, 116012 Dalian, China*
[c] *Institute of Physics, Chinese Academy of Sciences, Beijing 100080, China*

Received 8 June 2006; received in revised form 13 October 2006; accepted 26 October 2006
Available online 3 November 2006

Abstract

The charge transfer mechanism of a synthesized near-infrared (NIR) heptamethine cyanine dye has been studied with 3D real space analysis method. A new phenomenon about the intramolecular charge transfer (ICT) process is observed: the sulfonate ($-SO_3^-$) groups are mainly concerned with the ICT process. The electrons can transfer from the sulfonate ($-SO_3^-$) groups to the bridgehead amine and the electron-defect conjugated system. And the absorption and fluorescence spectra of the ICT state in alcoholic and aprotic solvents are analyzed. The spectral regularities are explained by the Kamlet and Taft (π^*, α, β) scale and the ICT mechanism. Specific hydrogen-bonding interactions between the solute and solvent are considered to explain the different spectral regularities of the dye in alcoholic and aprotic solvents.

Keywords: The charge transfer mechanism; The hydrogen bond; The heptamethine cyanine dye; The absorption and fluorescence spectra

1. Introduction

Heptamethine cyanine dyes employed as fluorescence labels and sensors of biomolecules in vivo [1] have attracted immense interest where a biological matrix exhibits the least absorption and autofluorescence background [2]. But some bottlenecks limit the complete utilization in biology study, e.g. the limited number of fluorophores, bad photostability, poor water solubility and small Stokes shift [3]. All of these can decrease the detection sensitivity to a great extent [4,5]. Therefore, the NIR dyes with better photophysical properties, especially with larger Stokes shift, are very promising for NIR fluorescence bioassays. Many works were done to modify the heptamethine cyanine dyes by chemical synthesis in order to obtain more advanced photochemical and photophysical properties [1,6,7,30].

The novel water-soluble near-infrared heptamethine cyanine dyes with C–N bond group substituted at cyclohexenyl bridge in heptamethine chain are synthesized in the previous paper [9]. And three features can be obviously seen in the spectra: a large Stokes shift (~140 nm), broad and fairly structureless fluorescence spectra, and no mirror image relationship between the absorption and fluorescence spectra. The intramolecular charge transfer is considered to account for these, which is confirmed by spectra experiments that the rate of the transfer from locally excited (LE) state to ICT state is lowered in viscous polar solvents and in strong acid conditions. More details can be found in Ref. [9] and its supporting information.

The ICT mechanism [10–15] is widely used to explain the molecular absorption and fluorescence spectral regularities. The electron donor and acceptor moiety are coexisted in one molecule. Upon electronic excitation to the S_1 state, the electron can transfer from the electron donor moiety to the acceptor moiety through the conjugated system. This process is usually accompanied by a structural change [10]. For example, in Coumarin 151, the lone pair electron of the electron donor nature on the amino group can transfer to the moiety of electron acceptor nature in the carbonyl group, which induces a large dipole moment change between the S_0 and S_1 states. Thus a large Stoke shift is observed, which strongly depends on the solvent polarity, making the coumarin family as the popular

* Corresponding author. Tel.: +86 411 84379293.
E-mail address: klhan@dicp.ac.cn (K.-L. Han).

1010-6030/$ – see front matter © 2006 Elsevier B.V. All rights reserved.
doi:10.1016/j.jphotochem.2006.10.027

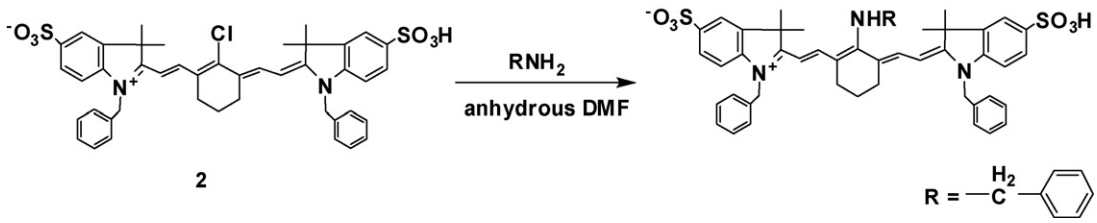

Fig. 1. Synthetic scheme for the heptamethine cyanine dyes.

probe molecules in time-dependent fluorescence measurements to study the solvation dynamics [10].

Undoubtedly, the solvent polarity can affect the photophysics of the solute [9], but site-specific interactions via hydrogen bonding between solute and solvent can strongly affect the photophysics of the dye molecule. So the study of the spectral properties of the dye in different solvent, especially in hydrogen-donating solvents, may provide more information about the utility in biology. In this work, we will further study the ICT mechanism of the novel dye by 3D real space analysis method. Moreover, the influence of the hydrogen-bonding interactions between the solute and solvent for the absorption and fluorescence spectral regularity is also considered.

2. Experimental

The heptamethine cyanine dyes containing robust C–N bond were synthesized from dye 2 by an apparent $S_{NR}1$ reaction (in Fig. 1). Briefly, dye 2 was stirred with RNH_2 in anhydrous DMF under argon at room temperature in the dark for 1 h. The product was purified on C18-RP column using methanol–water mixture as the eluent and characterized by spectroscopic data. More details about the synthesis of dye 2 can be found in Ref. [8]. The dye was solved at a concentration of 1.0×10^{-6} mol/dm^3 in solvents. The solvents are analytic reagents. Steady-state absorption and emission spectra of the dye in all solvents were recorded with a UV–vis absorption spectrophotometer (HP 8453, Hewlett–Packard Corp.) and a spectrofluorometer (C-700, Photon Technology International Corp.), respectively. All of the steady-state absorption and emission spectra were measured at room temperature.

3. Calculation method

The charge transfer of the dye was studied with 3D real space analysis method [16–20,27,29]. All the quantum-chemical calculations were done with Gaussian 03 suite [26]. The geometry optimizations of the dye were performed using density functional theory (DFT) [21] with Becke's three-parameter hybrid exchange function with Lee–Yang–Parr gradient-corrected correlation functional (B3-LYP functional) and 6-31G** basis set. No constrains to bonds/angles/dihedral angles were applied in the calculations and all atoms were free to optimize. The electronic transition energies and corresponding oscillator strengths were calculated with time-dependent density functional theory (TD-DFT) [22,23] at the B3LYP/6-31G** level [24,25].

4. Results and discussion

4.1. The ICT mechanism of the dye

The structural formulas of the heptamethine cyanine dye containing robust C–N bonds has been shown in Fig. 1. Two sulfonate groups in dye can provide a sphere of solvation in solvents, which brings better water solubility and can prevent the dye from aggregating [9]. The steady-state absorption and emission spectra of the dye are recorded in four alcoholic and three aprotic solvents, which can provide the useful information of the solute–solvent interactions in the ground and first excited singlet states. Typically, the steady-state absorption and fluorescence spectra of this dye in methanol are shown in Fig. 2.

From Fig. 2 it can be seen that no mirror image symmetry exists between the absorption and fluorescence spectra in dye (the half-widths of the absorption and fluorescence spectra are about 2756 and 1441 cm^{-1}, respectively), which indicates the change of geometry in the emitting and absorbing states [10,11]. This conclusion is confirmed by spectra experiments in the acid and viscous media [9]. In brief, the rate of the charge transfer from the LE state to ICT state is lowered in viscous polar solvents and the LE emission is dominant because the viscous polar solvent "coagulates" the geometry of the dye in the excited state. As a result the emission is only derived from the LE state. In protonation experiment, the LE emission phenomenon occurs again when pH is decreased because the geometry of a certain

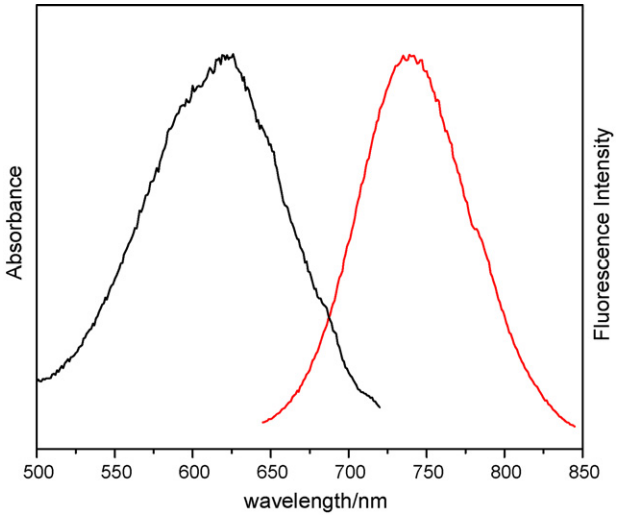

Fig. 2. The steady-state absorption (black) and fluorescence (red) spectra of the dye used in this paper in methanol.

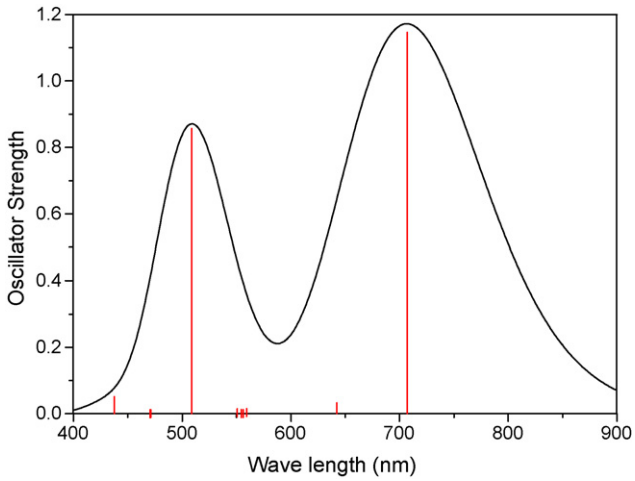

Fig. 3. The calculated absorption spectroscopy, where the full width at half-maximum of the Gaussian curves is set 3000 cm^{-1}.

site cannot change at the whole process due to the protonation in strong acid condition so as to the ICT emission disappears. (The more details can be found in Ref. [9].)

The 3D real space analysis method [16–20,27] is used to further study the ICT mechanism of the dye. Because the excited state properties are strongly influenced by the shapes of the frontier electronic level of individual monomer [27,28], the orbital densities of the HOMO and the LUMO of the individual dye molecule are studied in the process of the vertical absorption. In solution, a sulfonic group (–SO_3H) will be regarded as a sulfonate group and a proton. So the calculations are performed using (–SO_3^-)–(–SO_3^-) structure as the starting point. The calculated absorption spectrum of the dye is shown in Fig. 3, which is consistent with the experimental data [9]. In the UV–vis region, there mainly exist two absorption bands around the 509 and 707 nm, which are considered as the LE state and ICT state absorptions, respectively. But the calculated absorption spectrum is about 70 nm red shift compared to the experiment data perhaps due to the solvent effect in the real solution.

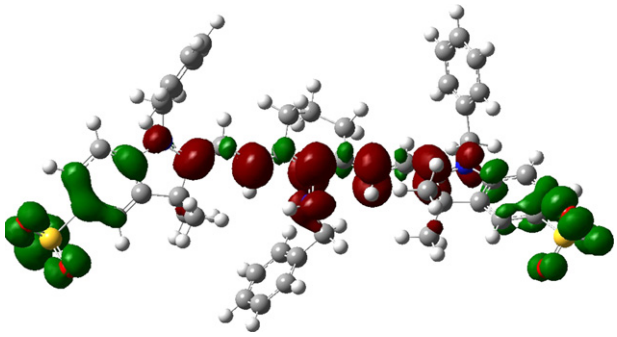

Fig. 4. The charge difference density in the vertical absorption for the ICT state of the dye. Green and red correspond to hole and electron for the charge difference density, and the isovalue is 4×10^{-4} a.u.

The spectra properties of the ICT state are more concerned because the ICT state spectrum can be observed in the common organic solvent but the LE state absorption disappears due to the fast charge transfer in solution [9]. From the calculations, the ICT state is mainly composed of HOMO-2 → LUMO and HOMO-8 → LUMO orbital transitions, and the CI main coefficients are 0.63496 and 0.13495, respectively. The calculated vertical absorption is 707.36 nm and the oscillator strength is 1.1343. The HOMOs and LUMOs are shown in Table 1.

The charge difference densities figure can visually express the characteristics of the electron–hole coherence and excitation delocalization in the vertical absorption. If there exists the ICT process, the site where the electron transfers from will be the hole (green) and the site where the electron transfers to will have the electron (red). If an atom does not involve in the charge transfer process, it will maintain neutrality, that is, no electron and hole. From the charge difference densities in the vertical absorption for the ICT state of the dye (Fig. 4), there does exist the charge transfer process during the excitation. But surpris-

Table 1
The HOMOs and LUMOs used in this paper, green and red correspond to the different phases of the molecular wave functions for the HOMOs and LUMOs, and the isovalue is 0.02 a.u.

	HOMOs		LUMOs
H-2	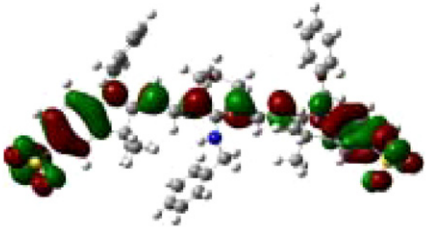	L	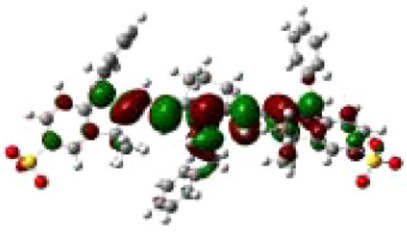
H-8	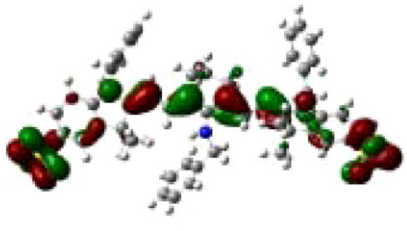		

Table 2
The steady-state absorption and fluorescence spectra, the Stokes shifts in alcoholic and aprotic solvents and Kamlet and Taft (π^*, α, β) solvent parameters used in the solvatochromic studies, which are taken from Refs. [10,33,34]

Solvents	Absorption λ_{ab} (nm)	Emission λ_{em} (nm)	Stokes shift (cm^{-1})	Kamlet and Taft scale		
				π^*	α	β
Methanol	623	740	2537	0.60	0.93	0.62
Ethanol	631	749	2497	0.54	0.83	0.77
1-Propanol	635	750	2415	0.52	0.78	0.80
2-Propanol	638	753	2394	0.48	0.76	0.95
DMSO	637	766	2644	1.00	0.00	0.76
DMF	644	767	2490	0.88	0.00	0.69
Acetone	657	766	2166	0.71	0.08	0.48

ingly, the calculations show that two sulfonate groups ($-SO_3^-$) are mainly concerned with the ICT process, which is originally designed to bring better water solubility and prevent the dye from aggregating [9]. As shown in Fig. 4, the electrons transfer from the sulfonate ($-SO_3^-$) groups to the electron-defect conjugated system and the bridgehead amine. Fortunately, the unexpected case will not change the viscous and protonation experiment phenomena because the viscous and strong acid conditions can coagulate the geometry of the sulfonate ($-SO_3^-$) and the bridgehead amine. When the electron transfers to the electron-defect conjugated system and the bridgehead amine.

4.2. The spectral properties of ICT state in solution

As well known, the Kamlet and Taft (π^*, α, β) scale provides a powerful approach to analyze the steady-state spectra and the Stokes shifts in the hydrogen-bonding system. In a series of papers [31–34], Kamlet and Taft measured the solvent polarity/polarizability parameter (π^*), the hydrogen bond donor (HBD) ability (α) and the hydrogen bond acceptor (HBA) ability (β). According to this model, a given steady-state absorption and fluorescence spectral observable XYZ can be parameterized as

$$XYZ = XYZ_0 + s\pi^* + a\alpha + b\beta \quad (1)$$

XYZ may be the peak or mean frequency of the steady-state absorption and fluorescence spectra. Where s, a and b are coefficients and XYZ_0 is the spectral frequency independent of solvent effects.

Intuitively, from the molecular structure of the dye, the benzene cycle, the oxygen atoms in sulfonate groups and the lone pair electron in the bridgehead amine can act as the hydrogen bond acceptors, moreover, the hydrogen atoms in the bridgehead amine can act as the hydrogen bond donors in the ground state. From the solvent aspect, the alcoholic molecule can provide the proton to form the hydrogen bond with the hydrogen bond acceptor in the dye; meanwhile, the alcoholic molecule can also accept the proton to form the hydrogen bond with the hydrogen bond donor in the dye. Thus, the alcoholic solvent shows amphipathy in the hydrogen-bonding system. For aprotic solvent, it can form the hydrogen bond with the hydrogen bond donor in the dye but cannot interact with the hydrogen bond acceptor. The hydrogen bonds, especially around the bridgehead amine and the sulfonate ($-SO_3^-$), are shown in Fig. 5 in the ground and excited states for the typical alcoholic and aprotic solvents, methanol and acetone.

We consider that the hydrogen bonds around the bridgehead amine and the sulfonates ($-SO_3^-$) are more important because these sites involve in the ICT process during the excitation, but the other sites do not so (Fig. 5). We expect that the geometry changes resulted from the charge density difference are reflected in the spectra and Stokes shifts. In aprotic solvent, the lone pair electron on the amine and the electron on the sulfonate ($-SO_3^-$) groups do not form the hydrogen bonds with solvents in both the ground and excited states (although there exists a very weak hydrogen bond between the electron and the hydrogen atom in acetone solvent, we consider that it is not important because of the very small α value). But in alcoholic solvent, the electrons on the amine and sulfonate ($-SO_3^-$) groups can form the hydrogen bonds with solvents in the ground state. It is well known that the lone pair electron on the $-NH_2$ group can accept a proton to ionize as $-NH_3^+$ form in acid medium, which lowers the conjugated ability of the lone pair electron with the π-cloud of the conjugated system [11]. As a result, the ionization causes the blue shift in the absorption spectrum for aniline [35]. In current experiment, the hydrogen bond will influence the bridgehead amine (–NHR) as the partly ionized form. As a result, it will be disadvantageous to accept the electrons transferred from the sulfonate ($-SO_3^-$) groups due to the decreased conjugated ability. For the sulfonate ($-SO_3^-$) groups, the hydrogen bond formed with the hydrogen atoms of the alcoholic solvents will hinder the participation of the electrons with the π-cloud of the conjugated system. As discussed above, these effects will increase the system energy, but cannot occur in aprotic solvent. As a result, the absorption spectra of the dye in alcoholic solvent shift to higher energy compared to those in aprotic solvent.

According to the Kamlet and Taft (π^*, α, β) scale, the parameter α represents the solvent hydrogen bond donor ability. If an alcoholic solvent has a bigger α value, the hydrogen bond (formed by the hydrogen atom in alcoholic solvent and the hydrogen bond acceptor in solute) will be stronger. From Table 2 it is clear that the strengths of the hydrogen bonds between the amino and sulfonate groups with the hydrogen atoms in alcoholic solvent decrease from methanol to 2-propanol. As a result, a red shift is found in the absorption spectra from methanol to 2-propanol. Our conclusions are supported by fitting the absorption spectral date with the Kamlet and Taft (π^*, α, β) scale. The

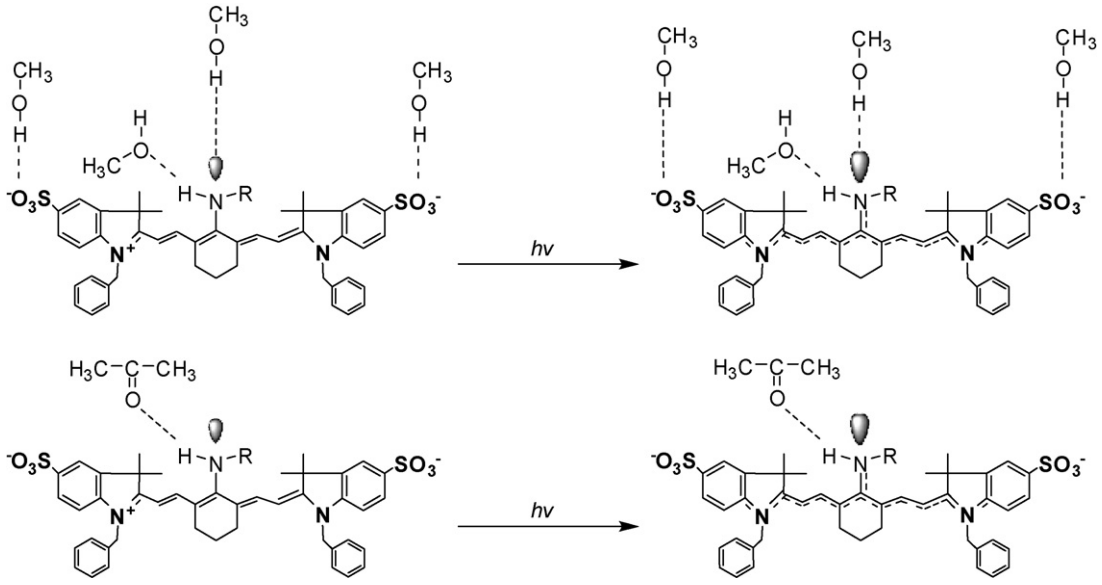

Fig. 5. Simplified view of the possible hydrogen bonds involved in the ground and excited states of the dye around the bridgehead amine and the sulfonate ($-SO_3^-$).

coefficients in Eq. (1) determined from these fits are given in Table 3. The calculated absorption data are plotted against the observed ones in Fig. 6.

From Table 3 the sign of the coefficient a is positive for the absorption spectra, which is consistent with our conclusion that the solvent hydrogen bond donor causes the blue shift in the absorption spectra. In addition, the coefficient a is almost ten times larger than the coefficient b, which indicates the hydrogen bond between the hydrogen bond donor in the dye with the oxygen atom in alcoholic solvent contributes little to the absorption spectra. From Fig. 6, it can be seen that all the points are almost on the diagonal line, which indicates that the regularity of the absorption spectra can be well explained using the Kamlet and Taft (π^*, α, β) scale.

For the fluorescence spectra of the dye, it can be also explained using the Kamlet and Taft (π^*, α, β) scale. The electrons in sulfonate groups will transfer to the electron-defect conjugated system and the amino in the excited state in both alcoholic and aprotic solvents. Although the hydrogen bonds between the amino and sulfonate groups with the hydrogen atoms in alcoholic solvent become weak in the excited state (the coefficient a decreases to 0.0612 as shown in Table 3), the solvent hydrogen bond donor ability still influences the charge transfer process by the hydrogen bonds [11]. The bigger α value the alcoholic solvent is, the less charge transfer is. In essence, the conjugations between the amino and sulfonate groups with the electron-defect conjugated system decrease in the dye, which causes the increase of the energy of the solute–solvent system in the excited state. As a result the shorter wavelength fluorescence is observed in methanol than that in 2-propanol in Table 1. Without this effect, the fluorescence spectra change slightly in aprotic solvent. Although the hydrogen bond acceptor ability (β) also contributes to the fluorescence spectra, it is still small since the coefficient a is about 2.6 times than b, which should not cause the fluorescence spectra to change greatly. A good correlation is also found as shown in Fig. 7.

The steady-state absorption and fluorescence spectra are well interpreted by using the Kamlet and Taft (π^*, α, β) scale and the ICT mechanism. Although the hydrogen-bonding interactions around the amino and sulfonate groups can account for the steady-state absorption and fluorescence spectra of the dye, it must note that, as discussed above, some hydrogen-bonding interactions in other sites can also contribute to the spectra slightly but they are not considered here.

Table 3
Coefficients of the relevant solvent parameters as defined by Eq. (1) (r = correlation coefficient)

	XYZ_0	s	a	b	r
Absorption data	1.3752	0.1852	0.1169	0.0157	0.99713
Fluorescence data	1.2831	0.0410	0.0612	−0.0236	0.99703

All the quantities in units of 10^4 cm^{-1}.

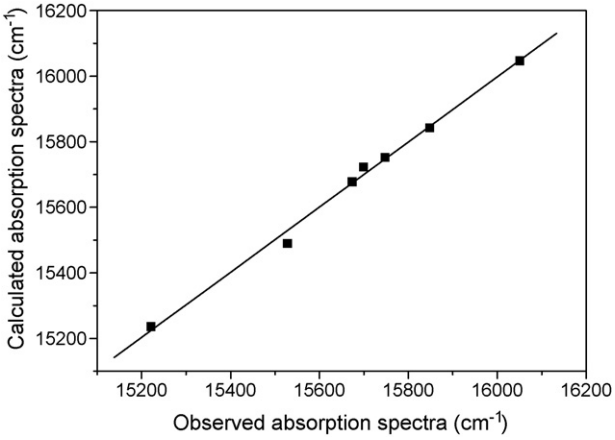

Fig. 6. Observed absorption spectra of the dye vs. calculated absorption spectra using the Kamlet and Taft (π^*, α, β) scale.

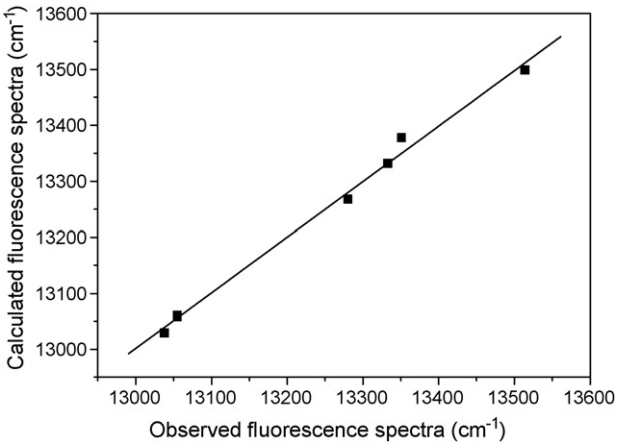

Fig. 7. Observed fluorescence spectra of the dye vs. calculated fluorescence spectra using the Kamlet and Taft (π^*, α, β) scale.

5. Conclusion

The charge transfer mechanism of a synthesized near-infrared heptamethine cyanine dye is studied with 3D real space analysis method. From the analysis of the charge difference densities in the vertical absorption for the ICT state of the dye, a new phenomenon about the ICT process is observed: the sulfonate ($–SO_3^-$) groups are mainly concerned with the ICT process, which is not considered in the previous paper. So the electrons can transfer from the sulfonate ($–SO_3^-$) groups to the bridgehead amine and the electron-defect conjugated system. The participation of the sulfonate ($–SO_3^-$) in the ICT process will not change the viscous and protonation experiment phenomena in the previous paper. Moreover, the ICT state absorption and fluorescence spectra are well explained by the Kamlet and Taft (π^*, α, β) scale. The hydrogen-bonding interactions between the solute and the solvent cause the different spectral regularities in alcoholic and aprotic solvents.

Acknowledgements

This work was supported by the National Natural Science Foundation of China (Grant 20403020). The authors are deeply appreciated to the help of Jian-Yong Liu and Ying Shi in experiment and discussions.

References

[1] A. Zaheer, R.E. Lenkinskl, A. Mahmood, A.G. Jones, L.C. Cantley, J.V. Frangioni, Nat. Biotechnol. 19 (2001) 1148–1154.
[2] M. Narayanan, G. Little, R. Raghavachari, J. Gibson, A. Lugade, C. Prescott, K. Reiman, D. Draney, Near-Infrared Dyes for High Technology Applications, Kluwer, Dordrecht, The Netherlands, 1998, pp. 141–158.
[3] S.A. Soper, Q.L. Mattingly, J. Am. Chem. Soc. 116 (1994) 3744–3752.
[4] L. Tolosa, K. Nowaczyk, J. Lakowicz, An Introduction to Laser Spectroscopy, 2nd ed., Kluwer, New York, 2002.
[5] Z. Zhang, S. Achilefu, Org. Lett. 6 (2004) 2067–2070.
[6] L. Strekowski, M. Lipowska, G. Patonay, J. Org. Chem. 57 (1992) 4578–4580.
[7] D.L. Gallaher, M.E. Johnson, Analyst 124 (1999) 1541–1546.
[8] F. Song, X. Peng, J. Photochem. Photobiol. A: Chem. 168 (2004) 53–57.
[9] X. Peng, F. Song, E. Lu, Y. Wang, W. Zhou, J. Fan, Y. Gao, J. Am. Chem. Soc. 127 (2005) 4170–4171.
[10] T. Gutavsson, L. Cassara, V. Gulbinas, G. Gurzadyan, J.-C. Mialocq, S. Pommeret, M. Sorguis, P. van der Meulen, J. Phys. Chem. A 102 (1998) 4229–4245.
[11] S.K. Saha, S.K. Dogra, J. Photochem. Photobiol. A: Chem. 110 (1997) 257–266.
[12] T.L. Arbeloa, F.L. Arbeloa, M.J. Tapia, I.L. Arbeloa, J. Phys. Chem. 97 (1993) 4704–4707.
[13] Z.R. Grabowski, K. Rotkiewicz, Chem. Rev. 103 (2003) 3899–4032.
[14] A.C. Benniston, A. Harriman, D.J. Lawrie, A. Mayeux, Phys. Chem. Chem. Phys. 6 (2004) 51–57.
[15] J.C. Jiang, C.E. Lin, J. Mol. Struct. (Theochem.) 392 (1997) 181–191.
[16] B.P. Krueger, G.D. Scholes, G.R. Fleming, J. Phys. Chem. B 102 (1998) 5378–5386.
[17] W.J.D. Beenken, T. Pullerits, J. Phys. Chem. B 108 (2004) 6164–6169.
[18] W.J.D. Beenken, T. Pullerits, J. Chem. Phys. 120 (2004) 2490–2495.
[19] N.K. Persson, M.T. Sun, P. Kjellberg, T. Pullerits, O. Inganäs, J. Chem. Phys. 123 (2005) 204718.
[20] M.T. Sun, J. Chem. Phys. 124 (2006) 054903.
[21] M.R. Dreizler, E.K.U. Gross, Density Functional Theory, Springer Verlag, Heidelberg, 1990.
[22] E.K.U. Gross, W. Kohn, Phys. Rev. Lett. 55 (1985) 2850–2852.
[23] R.E. Stratmann, G.E. Scuseria, M.J. Frisch, J. Chem. Phys. 109 (1998) 8218–8224.
[24] A.D. Becke, J. Chem. Phys. 98 (1993) 5648–5652.
[25] C. Lee, W. Yang, R.G. Parr, Phys. Rev. B. 37 (1988) 785–789.
[26] M.J. Frisch, et al., GAUSSIAN 03, Revision B. 05, Gaussian Inc., Pittsburgh, PA, 2003.
[27] M.T. Sun, Chem. Phys. 320 (2006) 155–163.
[28] J. Cornil, I. Gueli, A. Dkhissi, J.C. Sancho-Garcia, E. Hennebicq, J.P. Calbert, V. Lemaur, D. Beljonne, J.L. Brédas, J. Chem. Phys. 118 (2003) 6615–6623.
[29] M.T. Sun, T. Pullerits, P. Kjellberg, W.J.D. Beenken, K.L. Han, J. Phys. Chem. A 110 (2006) 6324–6328.
[30] K. Kiyose, H. Kojima, Y. Urano, T. Nagano, J. Am. Chem. Soc. 128 (2006) 6548–6549.
[31] M.J. Kamlet, J.L. Abboud, R.W. Taft, J. Am. Chem. Soc. 99 (1977) 6027–6038.
[32] M.J. Kamlet, C. Dickinson, R.W. Taft, Chem. Phys. Lett. 77 (1981) 69–72.
[33] M.J. Kamlet, J.L.M. Abboud, M.H. Abraham, R.W. Taft, J. Org. Chem. 48 (1983) 2877–2887.
[34] Y. Marcus, M.J. Kamlet, R.W. Taft, J. Phys. Chem. 92 (1988) 3613–3622.
[35] G. Kortum, Z. Physik. Chem. B 42 (1939) 39.